

# A 4% geometric distance to the galaxy NGC4258 from orbital motions in a nuclear gas disk

J. R. Herrnstein<sup>\*†</sup>, J. M. Moran<sup>†</sup>, L. J. Greenhill<sup>†</sup>, P. J. Diamond<sup>\*‡</sup>, M. Inoue<sup>§</sup>, N. Nakai<sup>§</sup>,  
M. Miyoshi<sup>¶</sup>, C. Henkel<sup>||</sup>, A. Riess<sup>\*\*</sup>

The accurate measurement of extragalactic distances is a central challenge of modern astronomy, being required for any realistic description of the age, geometry and fate of the Universe. The measurement of relative extragalactic distances has become fairly routine, but estimates of absolute distances are rare<sup>1</sup>. In the vicinity of the Sun, direct geometric techniques for obtaining absolute distances, such as orbital parallax, are feasible, but heretofore such techniques have been difficult to apply to other galaxies. As a result, uncertainties in the expansion rate and age of the Universe are dominated by uncertainties in the absolute calibration of the extragalactic distance ladder<sup>2</sup>. Here we report a geometric distance to the galaxy NGC4258, which we infer from the direct measurement of orbital motions in a disk of gas surrounding the nucleus of this galaxy. The distance so determined -  $7.2 \pm 0.3$  Mpc - is the most precise absolute extragalactic distance yet measured, and is likely to play an important role in future distance-scale calibrations.

NGC4258 is one of 22 nearby AGN known to possess nuclear water masers (the microwave equivalent of lasers). The enormous surface brightnesses ( $\gtrsim 10^{12}$  K), small sizes ( $\lesssim 10^{14}$  cm), and narrow linewidths (a few  $\text{km s}^{-1}$ ) of these masers make them ideal probes of the structure and dynamics of the molecular gas in which they reside. VLBI observations of the NGC4258 maser have provided the first direct images of an AGN accretion disk, revealing a thin, subparsec-scale, differentially rotating warped disk in the nucleus of this relatively weak Seyfert 2 AGN<sup>3,4,5,6</sup>. Two distinct populations of masers

---

<sup>\*</sup>National Radio Astronomy Observatory, PO Box O, Socorro, NM 87801

<sup>†</sup>Harvard-Smithsonian Center for Astrophysics, Mail Stop 42, 60 Garden Street, Cambridge, MA 02138

<sup>‡</sup>Merlin and VLBI National Facility, Jodrell Bank, Macclesfield, Cheshire SK11 9DL, U.K.

<sup>§</sup>Nobeyama Radio Observatory, National Astronomical Observatory, Minamimaki, Minamisaku, Nagano 384-13, Japan

<sup>¶</sup>VERA Project Office, National Astronomical Observatory, Mitaka, Tokyo, 181-8588, Japan

<sup>||</sup>MPIR, Auf dem Hugel 69, D-53121, Bonn, Germany

<sup>\*\*</sup>Department of Astronomy, University of California at Berkeley, Berkeley, CA 94720

exist in NGC4258. The *high-velocity* masers amplify their own spontaneous emission and are offset  $\pm 1000 \text{ km s}^{-1}$  and 4.7-5.1 mas (0.16-0.28 pc for a distance of 7.2 Mpc) on either side of the disk center. The beautiful Keplerian rotation curve traced by these masers requires a central binding mass ( $M$ ), presumably in the form of a supermassive black hole, of  $(3.9 \pm 0.1) \times 10^7 (D/7.2 \text{ Mpc})(\sin i_s / \sin 82)^{-2}$  solar masses ( $M_\odot$ ) where  $D$  is the distance to NGC4258 and  $i_s$  is the disk inclination. Because the high-velocity masers lie in the plane of the sky, they should to first order remain stationary as the disk rotates. The *systemic masers*, on the other hand, are positioned along the near edge of the disk and amplify the background jet emission evident in Figure 1<sup>12</sup>. A fundamental and as-yet untested prediction of the maser disk model is that the systemic masers should drift with respect to a fixed point on the sky by a few  $10 \mu\text{as yr}^{-1}$  as the disk rotates at  $\sim 1000 \text{ km s}^{-1}$ .

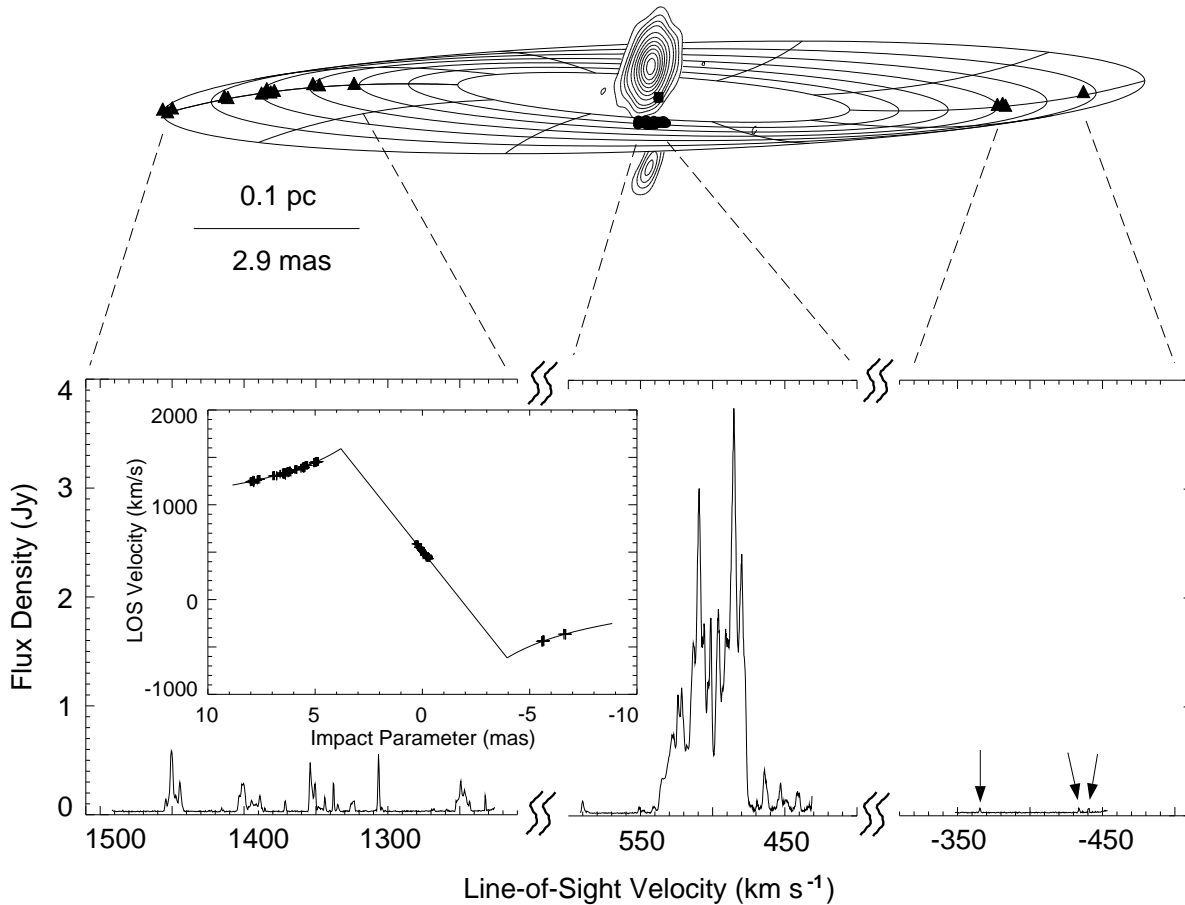


Fig. 1.— See captions at end of text.

NGC4258 was observed at 4–8 month intervals between 1994 and 1997 with the VLBA of the NRAO in order to search for the expected motions. Since the maser emission is essentially continuous across the envelope of systemic maser emission, we are forced to

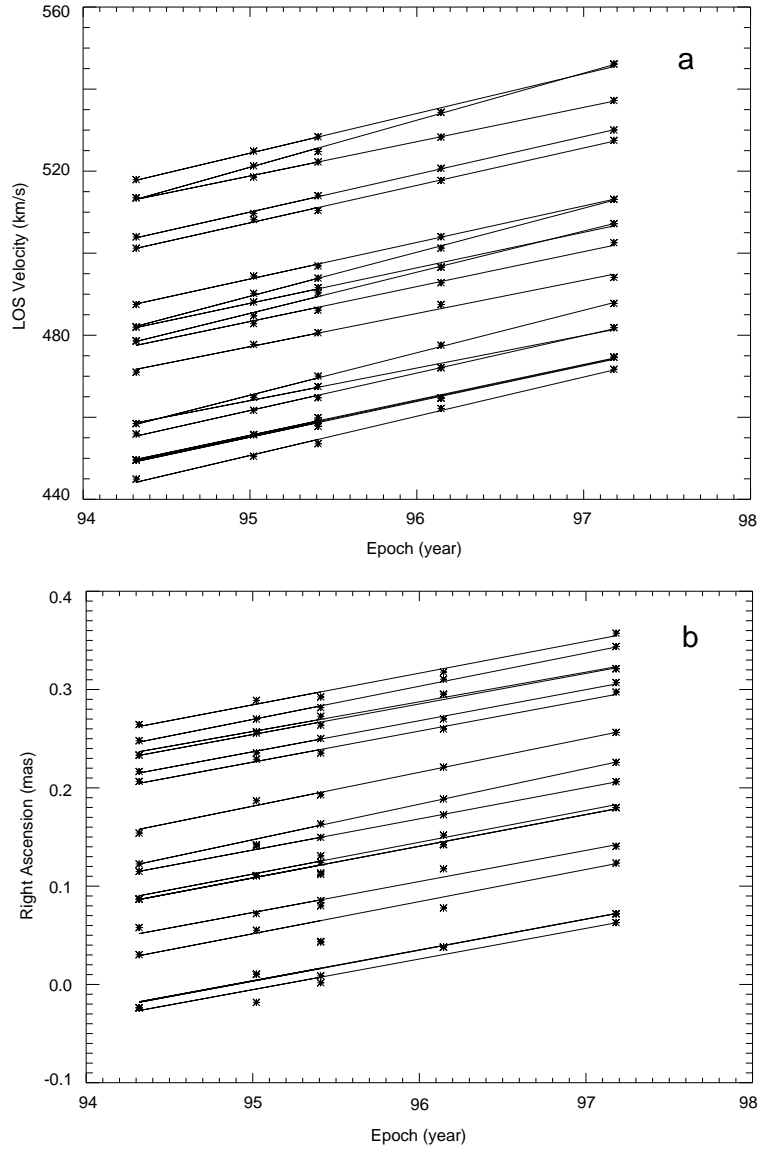


Fig. 2.— See captions at end of text.

rely on structure in the systemic spectrum to isolate and track individual maser features. The assumption that distinct peaks in the spectrum correspond to individual clumps of gas is justified by the successful tracking of maser accelerations in single-dish monitoring programs, and leads to an identification of 20–35 potentially trackable systemic masers in each epoch. These features are too densely packed in position and velocity to be individually tracked with any reliability. However, the resolution and sampling are sufficient to detect bulk rotation in the system, and we have developed a Bayesian pattern-matching analysis tool to track inter-epoch shifts in the positions and velocities of the systemic masers, as a whole<sup>7</sup>. The analysis assumes the systemic masers are randomly and narrowly scattered about an average radius,  $\langle r_s \rangle$ , of 3.9 mas, as indicated by the global disk-fitting analysis (see Figure 1). The precise magnitude of the radial scatter is set so as to maximize the overall likelihood of the tracking analysis. In order to evaluate the likelihood of a given bulk proper motion ( $\langle \dot{\theta}_x \rangle$ ) or acceleration ( $\langle \dot{v}_{los} \rangle$ ), the pattern-matching procedure must compute the likelihood that each individual maser has in fact moved by  $\langle \dot{\theta}_x \rangle$  or  $\langle \dot{v}_{los} \rangle$ . This leads to robust estimates for the “trackability” of each maser. Figure 2 shows the best-fitting acceleration and proper motion tracks for the most reliably trackable systemic masers. Figure 3 shows the overall probability density functions (PDFs) for  $\langle \dot{v}_{los} \rangle$  and  $\langle \dot{\theta}_x \rangle$ . The PDFs indicate a highly significant detection of bulk motion in the disk and from them we conclude  $\langle \dot{v}_{los} \rangle = 9.3 \pm 0.3 \text{ km s}^{-1} \text{ yr}^{-1}$  and  $\langle \dot{\theta}_x \rangle = 31.5 \pm 1 \text{ } \mu\text{as yr}^{-1}$ , where these and all subsequent uncertainties are  $1\sigma$  values. The latter result is consistent with expectations and is the first detection of transverse motion in the NGC4258 accretion disk. We note that the pattern-matching algorithm has been verified on a number of simulated datasets with feature densities and spectral and spatial resolutions comparable to those of the true data.

In order to convert the maser proper motions and accelerations into a geometric distance, we express  $\langle \dot{\theta}_x \rangle$  and  $\langle \dot{v}_{los} \rangle$  in terms of the distance and four disk parameters:

$$\langle \dot{\theta}_x \rangle = 31.5 \left[ \frac{D_6}{7.2} \right]^{-1} \left[ \frac{\Omega_s}{282} \right]^{1/3} \left[ \frac{\mathcal{M}_{7.2}}{3.9} \right]^{1/3} \left[ \frac{\sin i_s}{\sin 82.3^\circ} \right]^{-1} \left[ \frac{\cos \alpha_s}{\cos 80^\circ} \right] \text{ } \mu\text{as yr}^{-1}, \quad (1)$$

and

$$\langle \dot{v}_{los} \rangle = 9.2 \left[ \frac{D_6}{7.2} \right]^{-1} \left[ \frac{\Omega_s}{282} \right]^{4/3} \left[ \frac{\mathcal{M}_{7.2}}{3.9} \right]^{1/3} \left[ \frac{\sin i_s}{\sin 82.3^\circ} \right]^{-1} \text{ km s}^{-1} \text{ yr}^{-1}. \quad (2)$$

Here  $D_6$  is the distance in Mpc,  $\alpha_s$  is the disk position angle (East of North) at  $\langle r_s \rangle$ , and  $\mathcal{M}_{7.2}$  is  $M/D \sin^2 i_s$  as derived from the high-velocity rotation curve and evaluated at  $D = 7.2 \text{ Mpc}$  and  $i_s = 82.3^\circ$  (in units of  $10^7 M_\odot$ ).  $\Omega_s \equiv (G\mathcal{M}_{7.2}/\langle r_s \rangle^3)^{1/2}$  is the projected disk angular velocity at  $\langle r_s \rangle$  as determined by the slope of the systemic position-velocity gradient (in units of  $\text{km s}^{-1} \text{ mas}^{-1}$ ; see Figure 1). *a priori* estimates for each of these disk parameters, derived directly from the positions and velocities of the masers, are included in the denominators of each of the terms of equations 1 and 2.

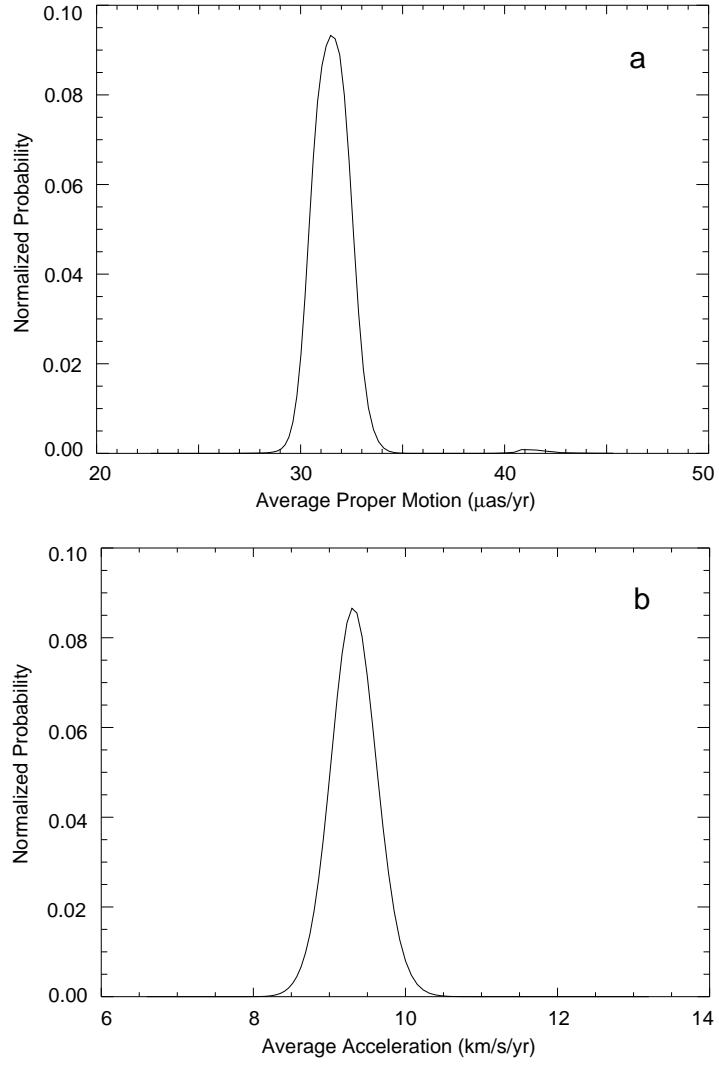


Fig. 3.— See captions at end of text.

When the *a priori* disk parameter estimates are used, the proper motions and accelerations yield independent distance estimates, through equations 1 and 2, of  $7.2 \pm 0.2$  Mpc and  $7.1 \pm 0.2$  Mpc, respectively. The quoted uncertainties are effectively the uncertainties in  $\langle \dot{\theta}_x \rangle$  and  $\langle \dot{v}_{los} \rangle$  recast in terms of distance, and as such are purely statistical in nature. The excellent agreement between the proper motion and acceleration distances for *a priori* values of the disk parameters is an impressive confirmation of the *a priori* disk model itself, and establishes the NGC4258 Keplerian disk as a fully self-consistent, dynamical model incorporating the positions, LOS velocities, proper motions, and accelerations of all the NGC4258 masers. We note that a preliminary geometric distance estimate, based on accelerations alone and a single VLBA epoch, yielded  $D = 6.4 \pm 0.9$  Mpc<sup>4</sup>. Hence, the old and new distances are consistent at the  $1\sigma$  level. The discrepancy between the estimates is ultimately explained by the fact that the original distance estimate assumed an average systemic maser radius about 10% larger than the value indicated by the newer data and the more sophisticated disk models.

Uncertainties in the disk parameters contribute to systematic uncertainties in the distance estimate. We derive a composite geometric distance estimate using equations 1 and 2, and from the  $\langle \dot{v}_{los} \rangle$  and  $\langle \dot{\theta}_x \rangle$  PDFs of Figure 3 and the *a priori* estimates for the disk parameters and their associated uncertainties. *The result is a geometric distance estimate of  $7.2 \pm 0.3$  Mpc, where the quoted uncertainty now incorporates all statistical terms associated with tracking motions in the disk as well as systematics arising from disk parameter uncertainties.* A  $\sim 5\%$  uncertainty in  $\Omega_s$  is the dominant contributor to the latter, producing fractional uncertainties in the acceleration and proper motion distances of 6.7% and 1.7%, respectively. In total, disk-model systematics contribute an additional 0.26 Mpc (in quadrature) to the distance error budget derived from purely statistical considerations.

The NGC4258 geometric distance is the most precise, absolute extragalactic distance measured to date and, being independent of all other distance indicators, it represents an important new calibration point for the extragalactic distance ladder. The geometric distance is consistent with pre-existing H-band Tully-Fisher ( $7.1 \pm 1.1$  Mpc<sup>16</sup>), blue Tully-Fisher ( $7.9 \pm 1.8$  Mpc<sup>17</sup>), and luminosity class ( $8.4 \pm 2.2$  Mpc<sup>18</sup>) distance estimates, all of which rely on the Cepheid Period-Luminosity relationship for absolute calibration. Most importantly, efforts are underway to determine directly a Cepheid distance to NGC4258 from Hubble Space Telescope (HST) observations of the galaxy. The NGC4258 geometric distance is presently the most precise means for directly calibrating distances obtained by HST Cepheid observations.

We emphasize that the above error budget considers statistical and systematic

uncertainties within the framework of a thin Keplerian disk in which the masers trace the orbital motions of discrete clumps of gas. As always, it is difficult to estimate any additional systematic uncertainties that might exist as a result of imperfections in the model itself. The potential impact of eccentricity on the distance error budget depends on the assumed distribution of accretion disk eccentricities in AGN in general. Viscous dissipation within such disks is expected to circularize orbits on relatively short timescales, and detailed modeling of the optical emission lines from a large sample of AGN suggests eccentricities less than about 0.5<sup>19</sup>. The eccentricity of the NGC4258 disk is further constrained by the symmetry of the maser emission about the disk center in both position and velocity<sup>12</sup>. These additional constraints lead to an expected eccentricity of zero with a probable error of 0.1, a negligible bias in the distance estimate, and a systematic uncertainty in the distance of 0.4 Mpc. Hence our distance estimate, including this uncertainty in the eccentricity, is  $7.2 \pm 0.5$  Mpc. Finally, we cannot unambiguously rule out contamination of the maser dynamics by some non-kinematical contribution, such as traveling density waves within the disk. However, given the complexity (30 systemic masers across  $8^\circ$  of disk azimuth) and the stability ( $\gtrsim 70\%$  of the features persisting) of the pattern we have tracked, orbital motion is certainly the simplest explanation.

## REFERENCES

1. Jacoby, G. H. *et al.* A critical review of selected techniques for measuring extragalactic distances. *PASP* **104**, 599–662 (1992).
2. Madore, B. F. *et al.* The Hubble Space Telescope Key Project on the Extragalactic Distance Scale. XV. A Cepheid distance to the Fornax Cluster and its implications. *Astrophys. J.* **515**, 29–41 (1999).
3. Watson, W. D. & Wallin, B. K. Evidence from masers for a rapidly rotating disk at the nucleus of NGC4258. *Astrophys. J.* **432**, L35–L38 (1994).
4. Miyoshi, M. *et al.* Evidence for a black hole from high rotation velocities in a sub-parsec region of NGC4258. *Nature* **373**, 127–129 (1995).
5. Greenhill, L. G., Jiang, R. D., Moran, J. M., Reid, M. J., Lo, K. Y., & Claussen, M. J. Detection of a subparsec diameter disk in the nucleus of NGC4258. *Astrophys. J.* **440**, 619–627 (1995).
6. Herrnstein, J. R., Greenhill, L. J., & Moran, J. M. The Warp in the subparsec molecular disk in NGC4258 as an explanation for persistent asymmetries in the maser spectrum *Astrophys. J.* **468**, L17–L20 (1996).
7. Herrnstein, J. R. PhD Dissertation, Harvard University, 1997.
8. Nakai, N., Inoue, M., Miyazawa, K., Miyoshi, M., & Hall, P. Search for extremely high velocity H<sub>2</sub>O maser emission in Seyfert galaxies. *Pub. Astron. Soc. Japan* **47**, 771–799 (1995).
9. Greenhill, L. J., Henkel, C., Becker, R., Wilson, T. L., & Wouterloot, J. G. A. Centripetal acceleration within the subparsec nuclear maser disk of NGC4258. *Astron. & Astrophys.* **304**, 21–33 (1995).
10. Bragg, A. E., Greenhill, L. J., Moran, J. M., & Henkel, C. Acceleration-derived positions of the high-velocity maser features in NGC4258. *BAAS.* **30**, 1254 (1998).
11. Moran, J. M. *et al.* Probing active galactic nuclei with H<sub>2</sub>O megamasers. *Proc. Natl. Acad. Sci. USA* **92**, 11427–11433 (1995).
12. Herrnstein, J. R. *et al.* Discovery of a subparsec jet 4000 Schwarzschild radii from the central engine of NGC4258. *Astrophys. J.* **475**, L17–L21 (1997).

13. Herrnstein, J. R. *et al.* VLBA continuum observations of NGC4258: Constraints on an advection-dominated accretion flow. *Astrophys. J.* **497**, L69–L73 (1998).
14. Cecil, G., Wilson, A. S., & DePree, C. Hot shocked gas along the helical jets of NGC4258. *Astrophys. J.* **440**, 181–190 (1995).
15. Zensus, J. A., Diamond, P. J., & Napier, P. J. *Very Long Baseline Interferometry and the VLBA* (Astr. Soc. Pacific, San Francisco, 1995).
16. Aaronson, M. *et al.* A catalog of infrared magnitudes and HI velocity widths for nearby galaxies. *Astrophys. J. Suppl.* **50**, 241–262 (1982).
17. Richter, O.-G. & Huchtmeier, W. K. Is there a unique relation between absolute (blue) luminosity and total 21 cm linewidth of disk galaxies? *Astron. & Astrophys.* **132**, 253–264 (1984).
18. Rowan-Robinson, M. *The Cosmological Distance Ladder* (W.H Freeman and Co., 1985).
19. Eracleous, M., Livio, M., Halpern, J. P., & Storchi-Bergmann, T. Elliptical Accretion Disks in Active Galactic Nuclei *Astrophys. J.* **438**, 610–622 (1995).

The National Radio Astronomy Observatory is a facility of the National Science Foundation operated under cooperative agreement by Associated Universities, Inc.

### CAPTIONS

Figure 1. – The upper panel shows the best-fitting warped disk model superposed on actual maser positions as measured by the VLBA of the NRAO, with top as North. The filled square marks the center of the disk, as determined from a global disk-fitting analysis<sup>7</sup>. The filled triangles show the positions of the *high-velocity* masers, so called because they occur at frequencies corresponding to Doppler shifts of  $\sim \pm 1000 \text{ km s}^{-1}$  with respect to the galaxy systemic velocity of  $\sim 470 \text{ km s}^{-1}$ . This is apparent in the VLBA total power spectrum displayed in the lower panel. The inset shows line-of-sight (LOS) velocity versus impact parameter for the best-fitting Keplerian disk, with the maser data superposed. The high-velocity masers trace a Keplerian curve to better than 1%. Monitoring of these features indicates that they drift by less than  $\sim 1 \text{ km s}^{-1} \text{ yr}^{-1}$ <sup>8,9,10</sup> and requires that they lie within  $5\text{--}10^\circ$  of the midline, the intersection of the disk with the plane of the sky. The LOS velocities of the *systemic* masers are centered about the systemic velocity of the galaxy. The positions (filled circles of upper panel) and LOS velocities of these masers imply they subtend about  $8^\circ$  of disk azimuth centered about the LOS to the central mass, and the observed  $8\text{--}10 \text{ km s}^{-1} \text{ yr}^{-1}$  acceleration of these features<sup>8,9</sup> unambiguously places them along the near edge of the disk. The approximately linear relationship between systemic maser impact parameter and LOS velocity demonstrates that the disk is very thin<sup>11</sup> (aspect ratio  $\lesssim 0.2\%$ ) and that these masers are confined to a narrow annulus in the disk. The magnitude of the velocity gradient ( $\Omega_s$ ) implies a mean systemic radius,  $\langle r_s \rangle$ , of 3.9 mas which, together with the positions of the high-velocity masers, constrains the disk inclination,  $i_s$ , to be  $\sim 82 \pm 1^\circ$  ( $90^\circ$  for edge-on). Finally, VLBA continuum images<sup>12,13</sup> are included as contours in the upper panel. The 22-GHz radio emission traces a sub-parsec-scale jet elongated along the rotation axis of the disk and well-aligned with a luminous, kpc-scale jet<sup>14</sup>.

Figure 2. – Line-of-sight (LOS) velocities (a) and right ascensions (b) at the peaks of the systemic maser spectrum for each of the five VLBA epochs. Only those features deemed reliably trackable by the pattern-matching analysis are included. All epochs included the Very Large Array, phased to act as a single large aperture. In addition, the final epoch utilized the Effelsberg 100-meter telescope. In each epoch the VLBA correlator provided cross-power spectra with channel spacings of  $0.22 \text{ km s}^{-1}$ . The NGC4258 masers are characterized by linewidths of  $\sim 1 - 3 \text{ km s}^{-1}$ . All spectra were phase-referenced, via self-calibration, to a strong systemic maser to stabilize the interferometer against atmospheric pathlength fluctuations, and synthesis images were constructed for each spectral channel using conventional restoration techniques<sup>15</sup>. Error bars have been foregone in order to avoid clutter. The uncertainties in individual LOS velocity estimates are dominated by line blending in the spectrum. There is an average scatter of about  $0.4 \text{ km s}^{-1}$  about the best-fitting acceleration tracks. The masers are spatially unresolved and relative

positions have been measured to a precision of  $\sim 0.5\Theta_B/\text{SNR}$ , where SNR is the signal to noise ratio and  $\Theta_B$  represents the  $0.6 \times 0.9$  mas, approximately North-South synthesized beam. Relative positional accuracies typically ranged from 0.5 to 10  $\mu\text{as}$ . All positions are relative to a fixed point along the systemic position-velocity gradient. Our ability to precisely align this structure amongst all epochs suggests that it does indeed remain fixed in time. The best-fitting acceleration and proper motion tracks (solid lines) indicate average drifts of  $9.3 \text{ km s}^{-1} \text{ yr}^{-1}$  and  $31.5 \mu\text{as yr}^{-1}$  in velocity and position, respectively. The scatter in the individual proper motions and accelerations about these average values is consistent with a 0.2 mas scatter in the radii of the systemic masers about  $\langle r_s \rangle$ .

Figure 3. – Systemic maser bulk proper motion ( $\langle \dot{\theta}_x \rangle$ ; a) and acceleration ( $\langle \dot{v}_{los} \rangle$ ; b) probability density functions (PDFs) as derived using the Bayesian pattern-matching analysis described in the text. The curves were generated using all the maser features in each epoch. The uncertainties in  $\langle \dot{\theta}_x \rangle$  and  $\langle \dot{v}_{los} \rangle$  as derived from these PDFs include measurement uncertainties in the maser positions and velocities, but they are dominated by ambiguities in tracking specific maser features.